PHYSICAL REVIEW B **79**, 045416 (2009)

Formation of an Au-Si eutectic on a clean silicon surface

A. L. Pinardi and S. J. Leake
London Centre for Nanotechnology, University College, Gower Street, London WC1E 6BT, United Kingdom

R. Felici
European Synchrotron Radiation Facility, 38043 Grenoble, France

I. K. Robinson
London Centre for Nanotechnology, University College, Gower Street, London WC1E 6BT, United Kingdom
and Diamond Light Source, Harwell Campus, Didcot OX11 0DE, United Kingdom

(Received 15 November 2008; revised manuscript received 6 December 2008; published 20 January 2009)

We investigated the formation of an AuSi eutectic from a silicon (100) surface cleaned under ultrahigh vacuum conditions and an evaporated 3-nm-thick gold layer using a suite of surface-sensitive x-ray techniques and Auger spectroscopy. The signature of the presence of the eutectic liquid came from its recently discovered surface-ordered state, whose diffraction pattern is confirmed. As expected, the eutectic started to form at its melting temperature (380 °C), but a small change in the film thickness was detected beforehand. The surface-ordered state was found to disappear at $T=473$ °C without the appearance of a second phase, but also to persist after resolidification of the liquid. Subsequent electron and x-ray microscopy after the sample was removed from vacuum showed the presence of phase-separated gold in the form of micronsized crystals on the surface.

DOI: 10.1103/PhysRevB.79.045416 PACS number(s): 61.05.C−, 61.30.Hn, 68.03.−g, 81.15.Ef

I. INTRODUCTION

One of the most interesting features of the gold-silicon binary phase diagram is their ability to form a very deep eutectic. The commonly accepted melting point of gold is $T_M(\mathrm{Au})=1063$ °C and the one of silicon is $T_M(\mathrm{Si})=1414$ °C. Though, for an alloy containing 18% Si and 82% Au, the melting point is as low as $T_E=359$ °C. This is called the eutectic point.[1]

Eutectics are very important in technology. Since it is usually much easier to melt a eutectic than a pure element, they are often used for soldering, where a liquid metal is needed to make a sound electrical contact. This particular eutectic is especially crucial because gold and silicon are often combined in electronic devices. However, direct contact between gold and silicon is usually avoided in commercial procedures because of degraded semiconductor properties if the eutectic is allowed to form during processing.

Moreover, eutectics are increasingly relevant in nanotechnology as they are used as catalysts in the growth of nanowires. The dimensions of a nanowire are so small that the behavior of atoms at the very surface becomes considerably important in determining the properties of such systems. An example of a practical application of a eutectic is the vapor liquid solid (VLS) method to grow nanowires:[2] at a fixed temperature higher than the eutectic temperature, there is an isolated environment with a substrate and some gold drops with a diameter of a few nanometers on top of it. With the use of the chemical vapor deposition (CVD) technique, a gas containing silicon is introduced in the environment. This gas deposits silicon onto the substrate and on the gold drops: if the temperature is high enough, gold and silicon form a eutectic liquid. As the silicon concentration continues to rise, the eutectic will reach saturation and silicon will start to precipitate in solid form below the liquid tip and a nanowire is created.[3]

A recent study on the AuSi eutectic was carried out by Shpyrko *et al.*[4,5] in Synchrotron Radiation experiments at Argonne and at Brookhaven. They presented evidence for the existence of a crystalline surface layer in a liquid gold-silicon alloy above the eutectic temperature. This phenomenon can be referred to as "surface freezing," which indicates the presence of a crystalline solid floating on top of a liquid sample.[6–8] This phenomenon of long-range lateral ordering is much more dramatic than the simple layering effect, typically two-three atomic layers thick, which is often present in liquid metals just above the melting point. Instead, Shpyrko *et al.*[4] assessed that in the AuSi case, the depth of this type of ordering is threefold greater than usually observed (i.e., around eight atomic layers). The evidence for this was seen with grazing incident x-ray diffraction scans as very sharp surface Bragg peaks present together with a broad peak, which is the hallmark of a liquid sample.

The second important discovery revealed by Shpyrko *et al.*[4,5] experiments was the presence of a solid surface first-order phase transition on increasing the temperature in the molten sample above 371 °C. This was observed as an extra set of solid surface Bragg peaks.

This paper describes the achievements and their understanding obtained in an experiment on a clean Si(100) sample, with a thin gold film evaporated on top. The experiment was carried out in ultrahigh vacuum (UHV) conditions and temperature was varied as the changes in the sample were tracked using various techniques. The goal was to observe the formation of the eutectic by direct reaction of gold and silicon under UHV conditions.

II. EXPERIMENT

The experiment was carried out at ID03, the surface diffraction beamline, at the European Synchrotron Radiation

Facility in Grenoble, France. A Si(100) sample was fixed onto a ceramic insulated sample holder by two tantalum clips. The clips were linked to a power supply so that current could pass through them and heat up the sample. A thermocouple was also attached to the clips, in order to keep track of the temperature changes. The sample was then introduced in a ultrahigh vacuum chamber to ensure a clean environment with a pressure of the order of 10^{-10} mbar.

Pure silicon in open air is protected by a thin layer of oxide which prevents contamination from any other material. Once introduced in the UHV chamber, the oxide was removed by temperature "flashes," taking care that the chamber pressure never exceeded 1×10^{-8} mbar. This widely used procedure allows a high temperature to be reached for a brief period of sublimation of the oxide before there is too much heating of the sample holder, which would cause outgassing and recontamination of the sample. During this procedure, we monitored the intensity and shape of a peak corresponding to the 1×2 reconstruction of the clean Si substrate. The temperature flashes were stopped when there was no further improvement of the 1×2 peaks. The highest temperature reached was 949 °C as read by the thermocouple. Then, 30 Å of gold was evaporated on top of the silicon held at room temperature, using a Knudsen cell evaporator attached to the chamber.

During the subsequent characterization, the temperature was slowly increased in steps of around 5 °C–30 °C up to 473 °C, well above the eutectic temperature. The sample was observed to become liquid at the interface at around T_E=380 °C. Note that only the interface where silicon comes in contact with gold became liquid due to eutectic properties: the bulk of the sample, which was pure silicon, remained solid due to its very high melting point.

The sample was cooled down and heated up once again, in order to investigate the reproducibility of the observations. Then, after taking many scans, the temperature was decreased to room temperature in order to allow for a new evaporation of extra gold on top of the sample. The sample was then heated again above the eutectic temperature T_E and cooled down once more. In this paper we will concentrate only on the analysis of the measurements made following the first evaporation.

Scans were taken on the sample with an x-ray beam of energy E=18 keV (λ=0.689 Å). The ID03 six-circle diffractometer was run in the "six-circle" mode.[9] Changes were tracked by different x-ray diffraction techniques, such as measurements of the reflectivity,[10] crystal truncation rod (CTR) scans,[11,12] and grazing incident diffraction (GID).[13] Some Auger spectroscopy scans were also taken with a Perkin-Elmer single-pass cylindrical mirror analyzer and 2 keV electron excitation. Each of these techniques was aimed to track and analyze a different aspect of the sample. Subsequently, *ex situ* scanning electron microscopy (SEM) and coherent x-ray diffraction (CXD) (Ref. 14) images of the sample were collected after the sample had been removed to air.

III. RESULTS

A. Surface-ordered layer

GID curves explored the features of the very last few monolayers of the surface: all our scans were taken at an incident angle smaller than the critical angle, since our goal was to achieve as much information as possible from the surface. Representative scans obtained at different stages of the experiment are presented in Fig. 1.

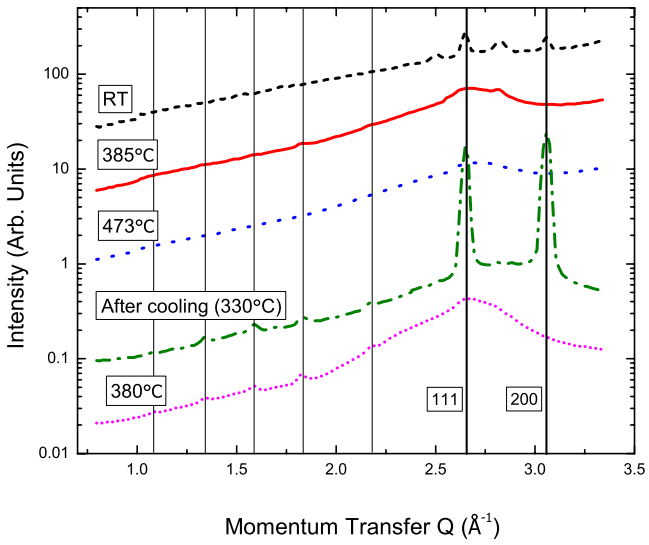

FIG. 1. (Color online) GID scans measured along an in-plane crystal direction that passes far from in-plane Bragg peaks. The black dashed line shows the sample at room temperature after the deposition (t=2118 min). The (red) solid line indicates the first melting, 2898 min after the gold evaporation, at T=385 °C. The (blue) dotted line was taken on the liquid sample at a higher temperature (T=473 °C, t=3522 min). The (green) dash-dotted line shows how the structure formed is frozen onto the surface once the sample is cooled back down to the solid states at t=4971 min and T=330 °C. The last scan, (purple) short dotted line, exhibits the melted sample after freezing to show the reproducibility of the results (T=380 °C, t=5285 min). The curves are displaced for clarity by multiplication by an arbitrary constant.

From the data of Fig. 1, three peaks emerged. (i) Contribution from (111) (Q=2.650 Å^{-1}) and (200) (Q=3.057 Å^{-1}) crystalline gold powder peaks; these were expected and observed as high intensity sharp peaks below the eutectic temperature on the frozen sample. (ii) A broad liquid peak, originating from short-range ordering of the gold and silicon atoms in the liquid form. We concluded that the sample's surface was liquid when this particular peak was seen in the scans. (iii) Solid surface peaks were observed as sharp moderately intense peaks at different angles along the whole GID scan.

Immediately after the deposition (black dashed scan) there is no evidence for the presence of a crystalline monolayer of the same form as the one obtained by Shpyrko, although there are traces of four different peaks. Two of them are clearly the (111) and the (200) gold powder peaks, whereas the other two visible peaks were not identified and would need further study to be fully understood. Our interpretation is that the sample is not yet completely annealed and that this is a transient state.

The GID scan after the first melting is shown as the solid red line in Fig. 1. Here, some of the most evident crystalline monolayer peaks predicted by Shpyrko are observed and highlighted by thin vertical lines. There is also the presence

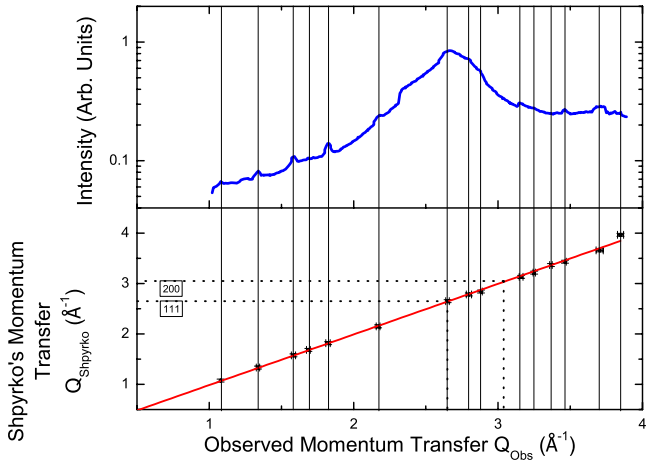

FIG. 2. (Color online) The upper box shows a GID scan which exhibits clearly the various positions of the crystalline surface peaks recorded at $t=3991$ min. In the lower box, the positions of the surface-ordered peaks Shpyrko measured are plotted against the ones we observed: the fitting line shows that the results are consistent and all but one peak coincide.

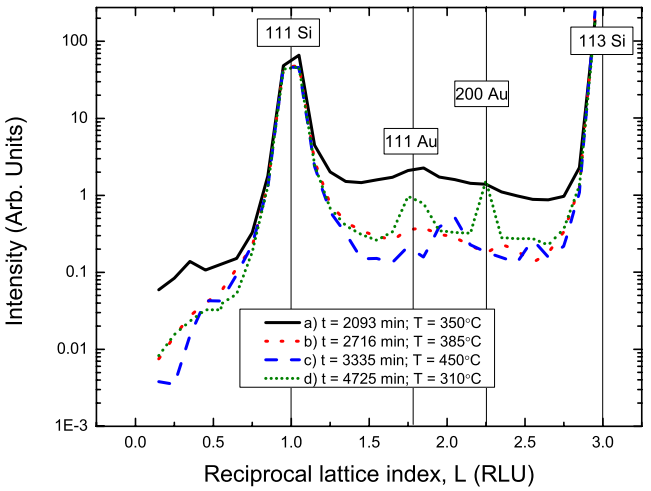

FIG. 3. (Color online) CTR passing through the silicon (111) and (113) bulk Bragg peaks. Integrated intensities have been background subtracted and corrected for instrumental geometry. The black solid scan represents room temperature before any manipulation; the (red) dot scan shows the melted sample at 380 °C; the (blue) dashed measurement was taken on the hot liquid sample at 450 °C; the (green) short dotted one shows the sample frozen back at 310 °C.

of a broad peak also seen in Shpyrko *et al.*'s[4,5] experiment, indicating the presence on an amorphous or short-range-ordered phase. This probably arises from the liquid phase at the melted sample's surface. Together these features are evidence that the crystalline layering on the surface exists on top of a melted film. Those peaks were observed to be present up to at least 450 °C. The next scan was taken at 473 °C by which point the ordered surface peaks have disappeared. The second phase observed by Shpyrko *et al.*,[5] with a different set of Bragg-peak positions, was not detected. While we confirm the presence of a surface-ordered state at $T>T_E$, the high-temperature phase was not seen. The peaks were observed at the same position at least up to $T=450$ °C and they disappeared beyond our detection sensitivity on the next scan at $T=473$ °C.

The presence of the crystalline layering peaks together with the (111) and the (200) gold Bragg peaks are proofs of the fact that the AuSi structure froze in the surface once the sample went back to the solid state at $T<T_E$. The last scan of Fig. 1 was taken when the sample was melted after the first manipulation, and it is shown here for two reasons: first of all, because it is a very clear image of the presence of a broad liquid peak together with the sharp peaks confirming Shpyrko's previous results; second, it is evidence for the reproducibility of the observations.

The positions in Q space of the sharp surface freezing peaks were extracted from Shpyrko *et al.*'s[4,5] paper and compared with our own values. Figure 2 shows the high degree of agreement between the two.

As we can see from Fig. 2, the values agree very well. Moreover, the slope of the fitting line is 1.0049, which shows an almost perfect agreement between the two structures. Since their diffraction patterns agree so well, we conclude that there is also a very good agreement between the lattice constants of the AuSi mixed structure. This fact strongly suggests that the surface structure obtained in our experiments starting from Si and Au and that of Shpyrko *et al.*[4,5] starting from a premixed alloy is the same.

B. Interface roughness

CTRs are mainly used in surface science to understand the structure of a crystal's surface.[11,12] Because the CTRs see only the boundary of the crystal whose reciprocal lattice is scanned, they are specific to that interface, even when it is buried under another structure.[12] In the present case, since gold was evaporated as powder on our Si(100) crystalline sample, when making CTR scans we were tracking the structure at the interface between the film and the substrate rather than at the surface. We can therefore use CTRs to see the roughness between the film and the crystal substrate.

Most of the scans were taken along the (11L) rod for $0.15\leq L\leq 2.99$. Silicon has a diamond lattice, hence due to selection rules the first two Bragg peaks along this rod were observed at (111) and (113). The intensity in between those peaks gives all of the information about the roughness of the interface: the smoother it is, the higher the intensity between the two Bragg peaks should be.

Figure 3 shows a comparison of four representative CTR scans in different states of heating. The measurements were taken at different times and at different temperatures. Note that together with the two Si Bragg peaks, also traces of gold powder rings were observed (green short dotted line). They originate from the fact that gold is polycrystalline at this stage of the experiment and hence contains a random distribution of orientations, some of which cross the CTR. These correspond to the Bragg angles of the (111) and the (200) peaks. Noticeably, the powder-diffraction peaks are seen to disappear on the liquid sample and to come back once the sample is frozen again. This agrees with the assumption that these peaks are a signature of the solidity of the gold.

The black solid line shows the CTR scans just after the deposition, and there may be a trace of the (111) gold peak

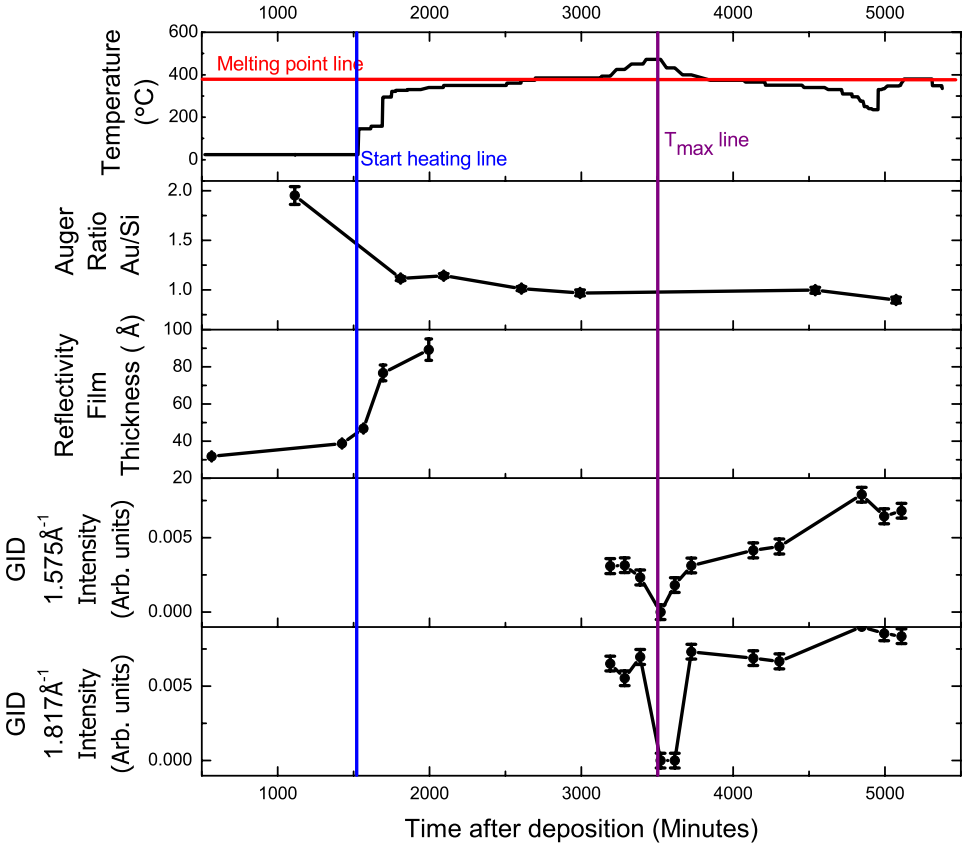

FIG. 4. (Color online) Time evolution of the various indicators of the state of the sample during the course of the experiment. The topmost box tracks the temperature changes that were made as a function of clock time; these were controlled by us by adjusting the current through the sample holder. The highest temperature reached was T_{max}=473 °C. The second box shows how the relative proportion of gold and silicon at the very surface changes, according to the Auger measurements obtained at different temperatures and times. The third box shows the increasing in the thickness of the noncrystalline layer as a function of temperature; this observation was extracted by the measurements of the reflectivity. The last two boxes show how the intensity of two different surface freezing peaks (respectively, the Q =1.575 Å^{-1} and the Q=1.817 Å^{-1} peaks for the fourth and the fifth boxes) changed as a function of time and temperature.

seen as a very diffuse crest. This suggests that the gold crystallites before any further manipulation are really small. According to the Scherrer formula, the size of the crystalline grain size is inversely proportional to the width of the peak. Here, the width is so broad and the peak is almost invisible. Hence the gold is in a very fine polycrystalline state immediately after the deposition.

The high intensity of the scan between the two Bragg peaks for the very first measurement shows that immediately after the evaporation of gold the Au-Si interface is quite smooth and flat. The red dot scan exhibits the sample slightly above the melting point (385 °C): the roughness is higher and the powder ring peaks disappear. The next measurement was taken on the liquid sample at 450 °C and it shows very high roughness and a feature which may be a Bragg peak of some sort of AuSi mixture. When the sample is cooled down and is frozen once again (green short-dotted line at 310 °C) the sample goes back to be a bit smoother (but not as much as just after the deposition) and the powder peaks return.

C. Auger and reflectivity

Comparison of all measurements taken together allows us to visualize the evolution of the sample state through the course of the treatments. This section explains most of the minor but still interesting results that were observed in the experiment. Figure 4 shows the results obtained with Auger scans, reflectivity measurements, and GID scans at different stages of the experiment.

The Auger ratio shows the relative peak-to-peak amplitude of the 69 eV gold peak and the 92 eV silicon peak in the dN/dE spectra. This ratio represents how the relative amount of gold and silicon at the very surface changes with time and temperature. The result shows a clear trend: in increasing the temperature, the amount of silicon at the surface increases well before the eutectic point. Moreover, on cooling down after melting, the silicon and the gold do not return to the original state of a uniform film covering the substrate: this is seen from the fact that when the sample is frozen after the thermal manipulation, the Au or Si parameter does not go back to the initial value, although the temperature conditions are very similar. This irreversibility is understood to be due to the formation of small gold islands occupying a fraction of the surface area, resulting in a similar Au or Si ratio to both the surface-ordered and disordered states of the liquid.

The measurements of the x-ray reflectivity[10] were used to obtain a value for the thickness of the gold film and also to

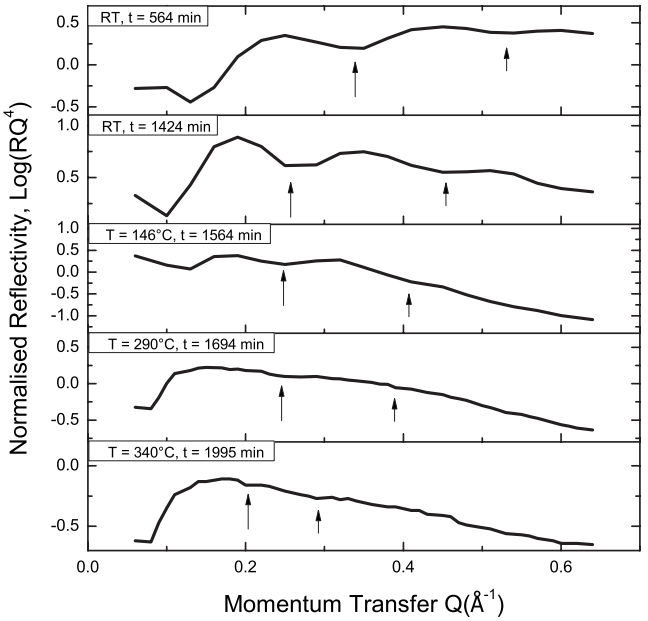

FIG. 5. Reflectivity measurements at different stages plotted against momentum transfer perpendicular to the surface. The topmost box in the stack shows the normalized reflectivity scan at room temperature just after the deposition. The second scan was taken one day later prior to heating. The third, the fourth, and the fifth boxes show scans at, respectively, 146°, 290°, and 340°: all of them prior to the first melting.

get a feeling for the evolution of the roughness of the film. Unlike the CTRs, the reflectivity reports the roughness of the outer surface density profile regardless of the chemical or crystalline state it is in.

The reflectivity measurements were mainly taken at the beginning of the experiment, while we were heating up the sample for the first time. Whenever the film has two well-defined boundaries, there are periodic oscillations in the reflectivity whose spacing is inversely proportional to the thickness of the film itself. The thickness of the film was calculated by extracting the minima of the oscillations. This procedure gave rise to a major source of error in finding the thickness of the film, especially because as the temperature was increased, the oscillations became less distinct. The third box of Fig. 4 shows how the thickness of the film increases with time and temperature. It is clear that the apparent thickness starts to increase before any melting takes place. This could be due to the onset of chemical mixing or the beginning of dewetting where the gold film becomes thicker in some parts and thinner (or disappears) in others.

Figure 5 shows plots of the reflectivity normalized to Fresnel reflectivity by multiplying it by Q^4 against the momentum transfer taken at different times. As the temperature was increased, the oscillations became much fainter. Taking a closer look, we also find that the peaks of the oscillations undergo a constant decrease in intensity with respect to the previous scan as the temperature is changed. This concept will be clear when observing, for instance, the line representing the first measurement and the one which pictures the third measurement. This peculiarity shows that the roughness is increasing rapidly with temperature and time.

The variation in the intensity of the two most prominent surface-ordered GID peaks (at $Q=1.575$ Å^{-1} and $Q=1.817$ Å^{-1}) was tracked as a function of time and temperature. The last two boxes of Fig. 4 represent another way to show evidence for the presence of the ordered surface peaks above the eutectic temperature and also of their disappearance at a higher temperature. At $T=473$ °C no solid phase on the surface is present anymore. The exact temperature at which these features vanish cannot be estimated precisely because of two reasons. First of all, there was a big error (about 10 °C) in the thermocouple due to its attachment on the sample clips. Its measurements were internally consistent during the experiment but not toward calibrated temperature values. Second, the measurements at high temperatures were not taken with very close steps.

The reproducibility of the surface-ordered phase is represented by the fact that the peaks return on cooling down the sample after disappearing at a high enough temperature. The peak at $Q=1.575$ Å^{-1} reappears straight away at 432 °C, while the one at $Q=1.817$ Å^{-1} returns at 400 °C. Again, at this stage, the scans were taken in steps of at least 15 °C–20 °C, so we do not aim to give an exact value for the temperature at which changes happen but just an idea of what happens. Moreover, if the temperature manipulation would have been slower, there is a possibility that both of the peaks tracked would have reappeared in the 432 °C scan. The lower the temperature, the more intense the peaks should be. The frozen sample shows evidence for the presence of the peaks, hence the surface structure formed on the melted sample is trapped into the sample.

IV. CONCLUSIONS

The confirmation of the observation of a distinct long-range-ordered solid phase floating on the eutectic liquid seen by Shpyrko *et al.*[4] is the main achievement of the experiment. The excellent agreement of the values of the peaks between our and Shyrko's experiments indicates that the AuSi structure formed is highly reproducible. We have used a very different UHV method of preparing the state rather than a premixed liquid. This makes it very unlikely to be caused by impurities, which would undoubtedly be different between the two methods.

The crystalline surface phase transition was not observed and this disagreement may arise from possible contamination in one of the two experiments or by the fact that above 430 °C we scanned at steps of around 15 °C–20 °C so we may have missed the phase change. This is not very likely though, since even considering a thermocouple error of 21 °C (which would allow for our eutectic temperature to be analogous to the one observed by Shpyrko), the possible phase-transition temperature should be below 400 °C.

Note that although our temperature calibration was very imprecise, what was important to us was the consistency of the thermocouple, which was satisfactory since the eutectic temperature was always observed at 380 °C.

SEM images of the sample taken after transfer through air are shown in Fig. 6. They exhibit a substrate with distinctly separated drop-shaped islands, presumably of pure gold. The

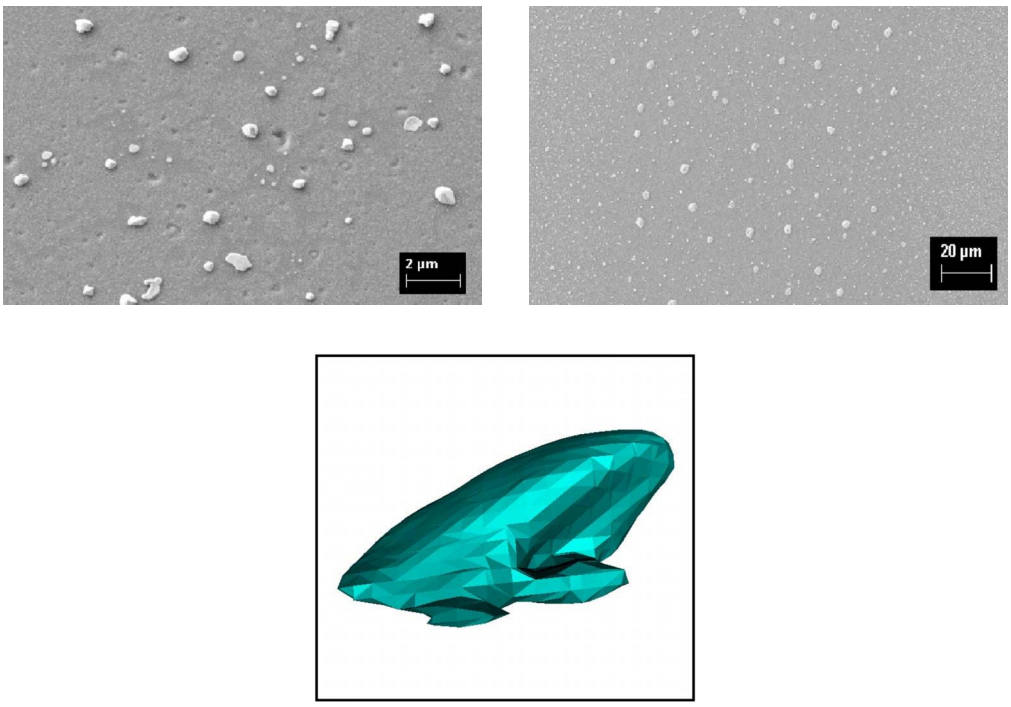

FIG. 6. (Color online) SEM and CXD images of the sample after it was removed from the vacuum system. The size of the CXD image is approximately 1 μm across.

SEM image on the left clearly shows some roughness of the substrate, in between the islands. Some holes have appeared where the drops may have become detached during manipulation of the sample. The SEM picture on the right shows the presence of a band of distinctly bigger drops, about 100 μm wide, which is about the same size as the x-ray beam at ID03. Since the x-ray beam was illuminating the sample in the same place during the heating and cooling cycles, it has apparently interfered with the nucleation of crystalline islands on the surface of the substrate. This could be due to direct beam heating or some nonthermal activation of the gold surface diffusion in the presence of the beam. It is not known at what stage during the experiment this redistribution of the gold took place; in our analysis above, we assumed a uniform thin-film sample format; but the gradual loss of fringes in the reflectivity may indicate that surface migration was already taking place during the first heating cycle.

The third panel in Fig. 6 shows an image obtained with CXD (Ref. 14) of one of the crystals on the surface. It shows an isosurface through the three-dimensional (3D) reconstructed density map of one of the islands. The strange shape seen with a round domed top and scalloped bottom suggests that the selected grain probably contained more than one crystalline domain. The CXD image was made from a single (111) Bragg reflection, which would not contain signals from the other domains making up the droplet.

Overall, the effect of the eutectic formation is clear in the results. The initial deposition was at $T < T_E$ where no intermixing of Au and Si takes place. Strong fringes in the x-ray reflectivity indicate a well-formed film with two flat sides. Gentle heating leads to only a slight thickening of the film which might be attributed to instability of the Au layer itself, becoming thicker in some places while thinner in others. The Auger ratio also changes here to show more Si, again possibly because of the thinned regions. Upon reaching $T = T_E \simeq 380$ °C a eutectic forms which is revealed by its characteristic GID pattern. The GID peaks, which index to the same structure seen by Shpyrko *et al.*,[4] were identified as laterally long-range-ordered solid layers floating on the liquid. Upon further heating, this ordered structure disappears by $T = 473$ °C without showing the second phase found before.[5] Upon cooling below T_E, the eutectic separates back into its components, which are seen as isolated islands in subsequent SEM and CXD experiments.

ACKNOWLEDGMENTS

We would like to thank the ID03 beamline staff, particularly Thomas Dufrane and Helena Isern, for their help during the experiment and the Royal Society and EPSRC-GB for supporting the research.

[1] B. Satpati, P. V. Satyam, T. Som, and B. N. Dev, Appl. Phys. A: Mater. Sci. Process. **79**, 447 (2004).
[2] R. S. Wagner and W. C. Ellis, Appl. Phys. Lett. **4**, 89 (1964).
[3] S. Kodambaka, J. Tersoff, M. C. Reuter, and F. M. Ross, Science **316**, 729 (2007).
[4] O. G. Shpyrko, R. Streitel, V. S. K. Balagurusamy, A. Y. Grigoriev, M. Deutsch, B. M. Ocko, M. Meron, B. Lin, and P. S. Pershan, Science **313**, 77 (2006).
[5] O. G. Shpyrko, R. Streitel, V. S. K. Balagurusamy, A. Y. Grigoriev, M. Deutsch, B. M. Ocko, M. Meron, B. Lin, and P. S. Pershan, Phys. Rev. B **76**, 245436 (2007).
[6] X. Z. Wu, B. M. Ocko, E. B. Sirota, S. K. Sinha, M. Deutsch, B. H. Cao, and M. W. Kim, Science **261**, 1018 (1993).
[7] B. Yang, D. Li, and S. A. Rice, Phys. Rev. B **67**, 212103 (2003).
[8] Z. Dogic, Phys. Rev. Lett. **91**, 165701 (2003).
[9] M. Lohmeier and E. Vlieg, J. Appl. Crystallogr. **26**, 706 (1993).
[10] J. Als-Nielsen and D. McMorrow, *Elements of Modern X-ray Physics* (Wiley, New York, 2001).
[11] I. K. Robinson and D. J. Tweet, Rep. Prog. Phys. **55**, 599 (1992).
[12] I. K. Robinson, Phys. Rev. B **33**, 3830 (1986).
[13] T. H. Metzger, I. Kegel, R. Paniago, and J. Peisl, J. Phys. D **32**, A202 (1999).
[14] M. A. Pfeifer, G. J. Williams, I. A. Vartanyants, R. Harder, and I. K. Robinson, Nature (London) **442**, 63 (2006).